

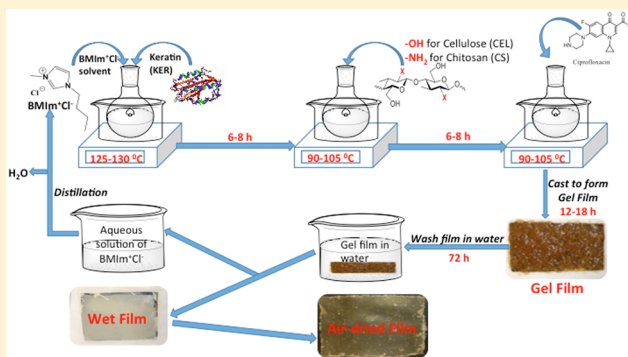
## Cellulose, Chitosan, and Keratin Composite Materials. Controlled Drug Release

Chieu D. Tran\* and Tamutsiwa M. Mututuvvari

Department of Chemistry, Marquette University, P.O. Box 1881, Milwaukee, Wisconsin 53201, United States

### S Supporting Information

**ABSTRACT:** A method was developed in which cellulose (CEL) and/or chitosan (CS) were added to keratin (KER) to enable [CEL/CS+KER] composites to have better mechanical strength and wider utilization. Butylmethylimidazolium chloride ([BMIm<sup>+</sup>Cl<sup>-</sup>]), an ionic liquid, was used as the sole solvent, and because the [BMIm<sup>+</sup>Cl<sup>-</sup>] used was recovered, the method is green and recyclable. Fourier transform infrared spectroscopy results confirm that KER, CS, and CEL remain chemically intact in the composites. Tensile strength results expectedly show that adding CEL or CS into KER substantially increases the mechanical strength of the composites. We found that CEL, CS, and KER can encapsulate drugs such as ciprofloxacin (CPX) and then release the drug either as a single or as two- or three-component composites. Interestingly, release rates of CPX by CEL and CS either as a single or as [CEL+CS] composite are faster and independent of concentration of CS and CEL. Conversely, the release rate by KER is much slower, and when incorporated into CEL, CS, or CEL+CS, it substantially slows the rate as well. Furthermore, the reducing rate was found to correlate with the concentration of KER in the composites. KER, a protein, is known to have secondary structure, whereas CEL and CS exist only in random form. This makes KER structurally denser than CEL and CS; hence, KER releases the drug slower than CEL and CS. The results clearly indicate that drug release can be controlled and adjusted at any rate by judiciously selecting the concentration of KER in the composites. Furthermore, the fact that the [CEL+CS+KER] composite has combined properties of its components, namely, superior mechanical strength (CEL), hemostasis and bactericide (CS), and controlled drug release (KER), indicates that this novel composite can be used in ways which hitherto were not possible, e.g., as a high-performance bandage to treat chronic and ulcerous wounds.



## INTRODUCTION

Keratins (KER) are a group of cysteine-rich fibrous proteins found in filamentous or hard structures such as hairs, wools, feathers, nails, and horns. Like other naturally derived protein biomaterials such as collagen, KER possess amino acid sequences similar to those found on extracellular matrix (ECM). Because ECM is known to interact with integrins which enable it to support cellular attachment, proliferation and migration, KER-based biomaterials are expected to have such properties as well.<sup>1-14</sup> In fact, KER extracted from human hair fibers was found to contain a cell adhesion motif of leucine-aspartic acid-valine (LDV)<sup>1</sup> and some regulatory molecules which, as a consequence, render it able to enhance nerve tissue regeneration. Keratin also exhibits minimal foreign body response and fibrous capsule formation.<sup>5</sup> The abundance and regenerative nature of wools and hairs coupled with the ability to be readily converted into biomaterials for the control of several biological processes have made KER a subject of intense study for various biomedical applications including scaffolds for tissue engineering and drug delivery.<sup>1-14</sup>

Unfortunately, in spite of its unique structure and properties, KER has relatively poor mechanical properties, and as a

consequence, materials made from KER lack the stability required for medical applications.<sup>1-14</sup> To increase the structural strength of KER-based materials, attempts have been made to cross-link KER chains with a cross-linking agent or convert its functional group via chemical reaction(s).<sup>1-14</sup> This rather complicated, costly, and multistep process is not desirable as it may inadvertently alter its unique properties, making the KER-based materials less biocompatible and diminishing its unique properties. A new method which can improve the structural strength of KER products not by chemical modification with synthetic chemicals and/or synthetic polymers but rather by use of naturally occurring biopolymers, such as cellulose (CEL) and/or chitosan (CS), is required.

Polysaccharides such as CEL are known to have strong mechanical properties.<sup>6-8</sup> Similar to CEL, CS, another polysaccharide derived from chitin, not only has strong mechanical properties but also has additional properties including its ability to stop bleeding (hemostasis), heal wounds,

**Received:** August 27, 2014

**Revised:** December 29, 2014

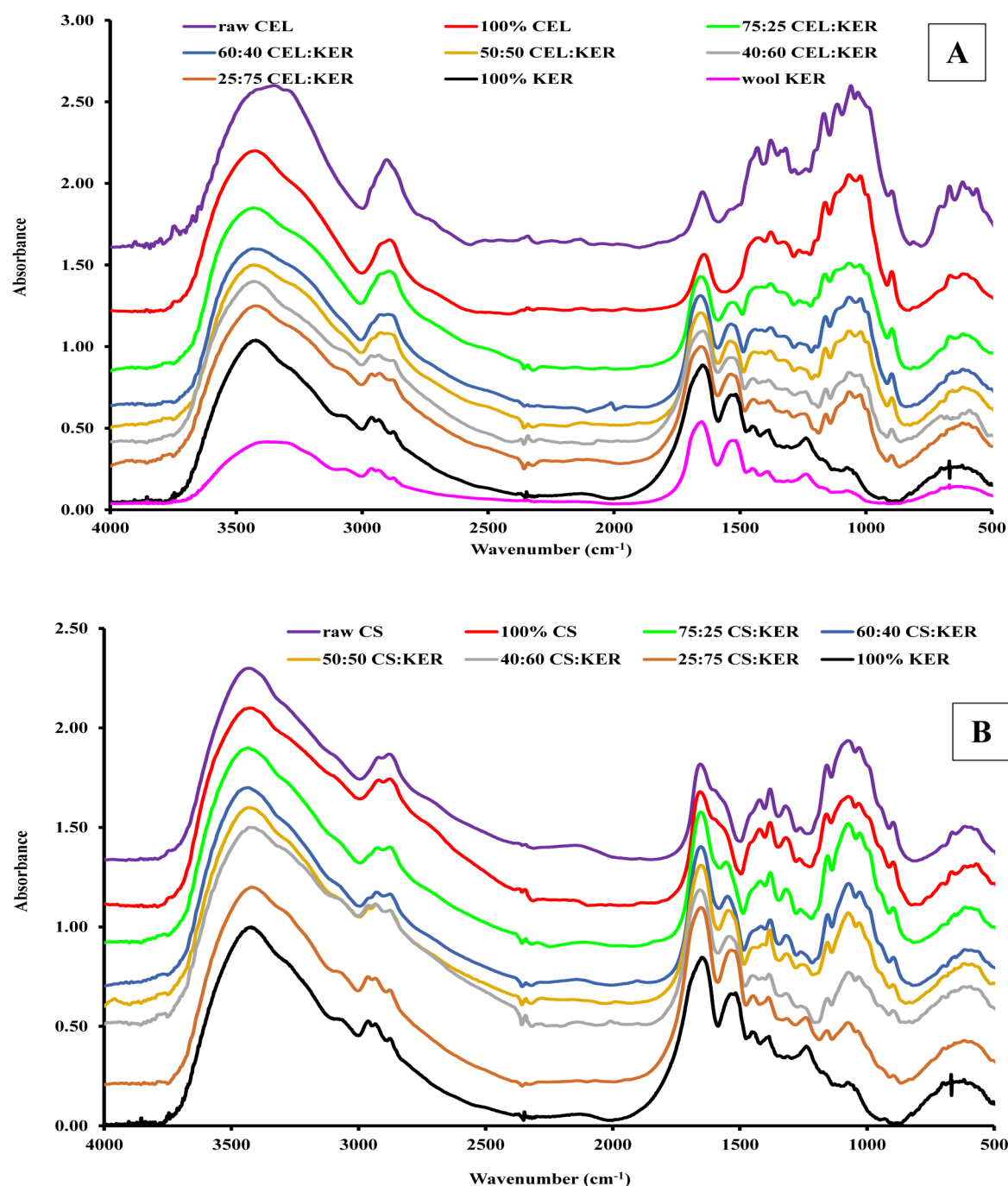
**Published:** December 30, 2014



Table 1. Kinetic Parameters of CPX Release Fitted to Different Kinetic Modes<sup>a</sup>

CS	% KER	CEL	zero-order model			first-order model			Higuchi model			Korsmeyer–Peppas model		
			$k_0$	$R^2$	MSC	$k_1$	$R^2$	MSC	$k_H$	$R^2$	MSC	$k_{SP}$	$n$	MSC
100			1.8(1)	0.9460	0.9469	2.7(1)	0.9731	1.8366	1.063(2)	0.9999	9.3389	1.06(1)	0.500(6)	8.9400
75	25		4(1)	0.8266	1.2521	6(2)	0.8788	1.6103	1.5(2)	0.9772	3.2792	1.10(6)	0.35(2)	5.1588
37.5	62.5		0.91(4)	0.9806	3.7409	1.36(4)	0.9938	4.8756	0.76(4)	0.9746	3.4721	0.82(2)	0.70(2)	5.2623
25	75		0.163(8)	0.9198	2.4752	0.265(8)	0.9663	3.3441	0.370(8)	0.9835	4.0579	0.313(5)	0.58(2)	2.4478
	100		0.29(2)	0.9668	3.2502	0.42(1)	0.9932	4.8381	0.43(2)	0.9789	3.7045	0.357(6)	0.72(3)	4.6356
	75	25	0.49(4)	0.9650	3.1034	0.74(2)	0.9938	4.8290	0.56(4)	0.9664	3.1444	0.53(1)	0.72(3)	4.4557
	25	75	2.3(4)	0.9433	2.3700	3.2(3)	0.9823	3.5359	1.16(6)	0.9944	4.6790	1.3(1)	0.62(6)	4.5319
	20	80	1.19(6)	0.9123	0.5700	1.98(5)	0.9740	2.1964	0.92(1)	0.9937	3.1844	1.13(2)	0.65(2)	4.9095
		100	0.93(6)	0.9129	0.2323	1.50(8)	0.9447	0.9290	0.92(2)	0.9973	4.0715	1.04(7)	0.60(5)	4.4566
25		75	2.0(2)	0.9275	0.6798	3.6(2)	0.9624	1.5482	1.42(2)	0.9991	5.2532	1.6(2)	0.57(6)	5.3904
50		50	2.1(2)	0.9185	0.3182	4.5(2)	0.9753	1.9323	1.53(2)	0.9997	6.2460	1.67(6)	0.54(2)	7.2202
75		25	2.0(2)	0.9342	0.8145	3.6(2)	0.9657	1.6932	1.35(3)	0.9981	4.4624	1.6(3)	0.6(1)	4.2671
50	10	40	1.8(1)	0.9504	1.0529	3.8(1)	0.9904	3.0892	1.17(7)	0.9857	2.6328	2.0(3)	0.77(8)	4.0657
40	20	40	0.73(2)	0.9642	1.5739	1.06(3)	0.9820	2.4761	0.62(1)	0.9967	3.8935	1.06(4)	0.55(2)	5.8134
30	30	40	1.29(6)	0.9749	1.8596	2.17(4)	0.9952	3.8445	0.86(3)	0.9886	2.7842	1.16(6)	0.62(2)	5.4192
20	40	40	0.117(4)	0.9084	0.1321	0.183(4)	0.9534	1.2089	0.317(3)	0.9978	2.7774	0.92(2)	0.53(4)	5.1612
10	50	40	1.02(6)	0.9321	0.4274	1.82(6)	0.9806	2.1153	0.97(1)	0.9984	4.3130	0.76(3)	0.43(2)	4.8179

<sup>a</sup>See text for detailed information.



**Figure 1.** FTIR spectra of (A) [CEL+KER] and (B) [CS+KER] composites. The spectra for CEL powder (panel A, purple curve) and CS powder (panel B, purple curve) are included for reference.

an additional 2 h. The viscous solution was then cast onto a Mylar film and left to undergo gelation at room temperature for 24 h. [BMIm<sup>+</sup>Cl<sup>-</sup>] was then removed by washing the gel film in 2.0 L of CPX-saturated water. Fresh CPX-saturated water was replaced every 24 h for 72 h. CPX-saturated water was used to minimize desorption of CPX from the film. The CPX-doped, [BMIm<sup>+</sup>Cl<sup>-</sup>]-free films were then air dried in a chamber with relative humidity controlled at around 60%. The same procedure was used to prepare composites with different compositions and concentrations of doped CPX.

**Procedure Used to Measure in Vitro Release of Ciprofloxacin from CPX-Doped [CEL+CS +KER] Composites.** In vitro CPX release from the CPX-doped composite films was monitored by the fluorimetric method. Essentially, about 3.0–3.5 mg of composite film, cut into a rectangular shape ( $4.3 \pm 0.2$  mm (L)  $4.1 \pm 0.3$  mm (W)

$0.18 \pm 0.02$  mm (thickness)), was placed in a standard 10 mm fluorescence cell. A PTFE mesh, cut to fit in the cell, was laid flat on top of the composite film. A tiny stir bar (7 mm  $\times$  2 mm  $\times$  2 mm, L  $\times$  W  $\times$  H) was then placed on top of the mesh. Exactly 3.5 mL of 1.0 mM phosphate buffer at pH 7.2 was added into the cell. The cell was closed with a stopper before being immediately inserted into the spectrofluorometer (QuantaMaster 40, PTI, Birmingham, NJ). The release of CPX was then monitored by recording emission spectrum of CPX in the buffer solution from 350 to 520 nm with  $\lambda_{\text{exc}} = 324$  nm. The emission spectrum was taken at specific time intervals for 10 h. The samples were then left to stir for additional 14 h before the last measurement was taken. This final measurement was used as the amount of CPX released at equilibrium. The amount of CPX released at each time point,  $M_t$ , was calculated by using a calibration curve



generated at  $\lambda_{\text{emis}} = 418$  nm. A preliminary experiment was carried out using a blank film (that is, a sample without CPX) to determine if [CEL+CS+KER] composites have any background signal. No background signal was detected. Additional experimentation was also performed to determine if CPX was stable during the 24 h measurement period. Fluorescence of a buffer solution containing CPX whose concentration was the same as that of CPX released at equilibrium was measured and monitored for 24 h. It was found that within experimental error, the fluorescence intensity remained the same throughout the whole period, which indicates that CPX was stable during the 24 h releasing measurement time.

**Kinetics of Drug Release.** The in vitro drug release data were fitted to four different kinetic models: zero-order,<sup>27,28</sup> first-order,<sup>27–30</sup> Higuchi,<sup>31,32</sup> and Korsmeyer–Peppas or power law model.<sup>33–36</sup> The zero-order model is based on the assumption that the rate of drug release is independent of its concentration. It is represented by the equation

$$\frac{M_t}{M_\infty} = k_0 t \quad (1)$$

where  $M_t/M_\infty$  is the fractional release of the drug at time  $t$  and  $k_0$  is the zero-order constant.

The first-order model describes a system in which the release rate is concentration-dependent; it is represented by the equation

$$\ln\left(1 - \frac{M_t}{M_\infty}\right) = -k_1 t \quad (2)$$

where  $k_1$  is the first-order rate constant.

Higuchi model, sometimes referred to as the square root law because of the square root of time dependence of drug released, is based on Fickian diffusion of the drug from the matrix.<sup>31,32</sup> This relation is taken to be valid during the early times of drug release, namely the time up to 60% release of the drug.<sup>31,32</sup> Because not all systems can be described by the Higuchi model, a more general model, the Korsmeyer–Peppas model,<sup>33–36</sup> was developed to describe all cases including systems which deviate from Fickian diffusion. The model relates fractional release to time through an empirical exponent,  $n$ , and rate constant,  $k_{\text{sp}}$ , according to

$$\frac{M_t}{M_\infty} = k_{\text{sp}} t^n \quad (3)$$

As expected, data fitted using this relation in the early time release region is the same as in the Higuchi model.<sup>31–36</sup> According to this model, the  $n$  exponential value is related to the mechanism of drug release.<sup>33–36</sup> Specifically, the release is Fickian diffusion when  $n \leq 0.45$ . If  $0.45 \leq n \leq 0.8$ , it indicates anomalous (non-Fickian) transport, and for  $0.8 \leq n \leq 1$ , the release follows case II, zero-order mechanism.<sup>33–36</sup>

Release of CPX by each composite was measured at least three times. Data obtained were fitted into the four different kinetic models described, and averaged kinetic parameters (rate constants ( $k_0$ ,  $k_1$ ,  $k_{\text{H}}$ , and  $k_{\text{sp}}$ ) and exponential  $n$  values) are reported together with their associated standard deviations. It is not possible to present all averaged rate constants together with their corresponding standard deviations because of space limitation of Table 1. As a consequence, the standard deviations are presented in the parentheses next to their corresponding averaged values. For example,  $k_{\text{sp}}$  for 100% CS is  $1.06 \pm 0.01$ , which is presented in Table 1 as 1.06(1).

## RESULTS AND DISCUSSION

**Spectroscopic Characterization.** Fourier transform infrared (FTIR) spectroscopy was used to confirm that CEL, CS, and KER were not chemically altered by dissolution with and regeneration from ionic liquids. Spectra of wool, shown as the pink curve in Figure 1A,B, exhibited characteristic bands that can be assigned to the vibrational modes of peptide bonds in proteins. For example, the bands at  $1700\text{--}1600\text{ cm}^{-1}$  and  $1550\text{ cm}^{-1}$  are due to amide C=O stretch (amide I) and C–N

stretch (amide II) vibrations, respectively.<sup>37</sup> In addition, the  $3280\text{ cm}^{-1}$  band can be assigned to N–H stretch vibration (amide A) while a band at  $1300\text{--}1200\text{ cm}^{-1}$  is due to the in-phase combination of the N–H bending and the C–N stretch vibrations (amide III). This finding is expected because wool contains more than 95% of keratin protein.<sup>38</sup> It is noteworthy to add that the FTIR spectrum of wool does not have any band at  $1745\text{ cm}^{-1}$ , which is known to be due to lipid ester carbonyl vibrations.<sup>39</sup> It seems, therefore, that the Soxhlet extraction effectively removed all residual lipids from wool. Interestingly, upon regenerating KER film from the wool, no new IR signatures were detected in the FTIR spectrum of the former (compare pink spectrum for wool to the black spectrum for 100% KER). The results indicate that dissolution by and regeneration of KER from [BMIm<sup>+</sup>Cl<sup>−</sup>] do not produce any chemical alteration in the chemical structure of KER.

The FTIR spectra of [CEL+KER] and [CS+KER] composites with different compositions are also presented in panels A and B of Figure 1, respectively. As expected, the spectra of these composite films exhibit bands characteristic of their respective components. Furthermore, magnitude of these bands seems to correlate well with the concentration of corresponding component in the film. For example, the band between  $900$  and  $1200\text{ cm}^{-1}$  (due to sugar ring deformations) increased in relative intensity concomitantly with the relative concentration of CEL in the [CEL+KER] composite (Figure 1A). On the other hand, the intensity of the amide I and amide II bands increased with the increase in the relative concentration of KER in the same composite films. Similar behavior was also observed for [CS+KER] composite films (Figure 1B). It is noteworthy to add that in all composite films ([CEL+KER], [CS+KER], and [CEL+KER+CS]), no new bands are found in their FTIR spectra, i.e., the spectra of the composites are a superposition of the spectra of the corresponding individual components. This, as noted earlier, further confirms that no chemical alterations occurred during the synthesis of these composites.

**Mechanical Properties.** Although KER has been shown to induce controlled release of drug substances,<sup>5,8,9,13</sup> its poor mechanical properties continue to hamper its potential applications. For example, as previously reported and also observed in this study, regenerated KER film was found to be too brittle to be reasonably used in any application. Because CEL is known to possess superior mechanical strength, it is possible to enhance the mechanical properties of KER-based composites by adding CEL or other polysaccharides such as CS into it. Accordingly, [KER+CEL] and [KER+CS] composites with different concentrations were prepared, and their tensile strength was measured. Figure 2 plots tensile strength of [CEL+KER] and [CS+KER] composites as a function of CEL and CS content. As illustrated, the tensile strength of [CEL+KER] composite films was found to increase concomitantly with the content of CEL. For example, the tensile strength of [CEL+KER] increased at least 4-fold when CEL loading was increased from 25% to 75%. This behavior has also been reported elsewhere when CEL was used as a reinforcement in other composites.<sup>16</sup> It is worth noting that [CEL+KER] composite films were much weaker than [CS+CEL].<sup>24</sup> For example, [CEL+KER] and [CEL+CS] containing 75% and 71% CEL had tensile strengths of  $36 \pm 3$  and  $52\text{ MPa}$ , respectively. This could be attributed to the fact that CEL structure is more similar to that of CS than KER structure. Therefore, interactions formed between CEL and CS can be much

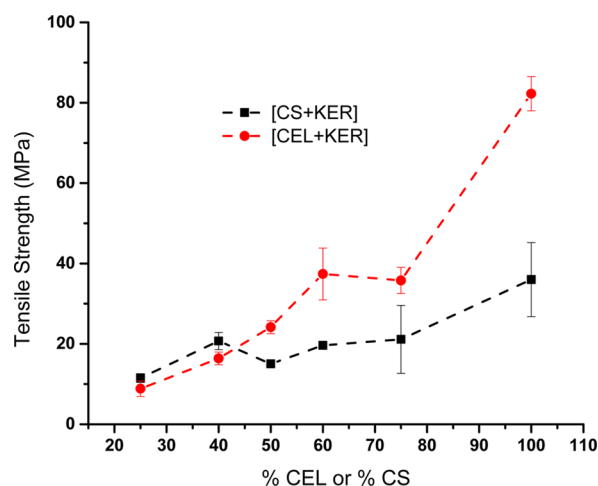


**Figure 2.** Plots of tensile strength as a function of % CEL in [CEL+KER] composites (red circles) and % CS in [CS+KER] composites (black squares).

stronger than those between CEL and KER. Although CS also leads to an increase in the tensile strength of [CS+KER], its effect is noticeably weaker than that of CEL of comparable loading. For example, [CEL+KER] and [CS+KER] had tensile strength values of  $37 \pm 6$  and  $20 \pm 1$  MPa, respectively, for a 40% KER loading. This could be due to the fact that CS has mechanical strength that is relatively inferior to that of CEL, which can be seen by the tensile strengths of 100% CS ( $36 \pm 9$  MPa) and 100% CEL ( $82 \pm 4$  MPa).

**Qualitative Assessment of the Release Assay.** The objective of this study was to evaluate if composites containing CEL, KER, and/or CS are suitable as matrix platforms for controlling the release of the drug CPX; if they are, an additional objective is determining the most effective composition and concentration of the composite. Drug release assays were carried out using composites containing relatively different concentrations of CEL, KER, and CS. The concentration of the drug was fixed at 0.5% of the total weight of the biopolymers in each formulation. Careful consideration was made to ensure that sink conditions for the drug were maintained throughout the experiment so that the release medium was not saturated by the released drug. Specifically, experimental conditions were chosen to ensure that the drug

concentration was always less than 10% of the saturation solubility in the release medium, which for CPX in phosphate buffer is  $73 \pm 7$  ppm at  $21 \pm 1$  °C.<sup>40</sup> Each of the composite films used in release experiments (i.e., 3.5 mg of film) contains 0.0174 mg of CPX (equivalent to 0.5% CPX per total weight of biopolymers in the composite) which in 3.5 mL of release medium corresponds to  $\sim 5$  ppm of the maximum concentration of CPX that can possibly be released by a typical composite film. Because this value is well below the CPX maximum solubility of  $73 \pm 7$  ppm, it is clear that sink conditions were maintained in this study.

Fluorescence spectra of the drug release from 100% KER film (i.e., CPX in solution) plotted as a function of releasing time are shown in Figure 3. As illustrated, the intensity of the fluorescence spectrum increases as a result of CPX being released into the buffer medium. The fact that the position of  $\lambda_{\text{max}}$  (at 480 nm) and the shape of the spectra remained the same throughout the entire release time seems to indicate that the drug remained stable over the whole assay period. In addition, these time-dependent spectra appeared to be identical to the calibration spectra (*not shown*). This suggests that CPX remained chemically stable throughout the encapsulating process into the biopolymer matrices.

Fluorescence spectra of CPX that were released from other films, 100% CS and 100% CEL, were also measured, and the results obtained were used, together with those for 100% KER, to generate plots of fraction of drug released,  $M_t/M_\infty$ , against time,  $t$ , for each film (Figure 4). As illustrated, for all three films, the release profiles are characterized by an initial rapid release that eventually reaches a plateau. While the duration and amount of CPX released are somewhat similar for 100% CS and 100% CEL, they are much different from those for 100% KER. For example, it took ca. 30 min for 100% CEL and 100% CS to release 60% of the encapsulated CPX, whereas up to a 4-fold greater time (120 min) was needed for 100% KER to release a similar amount of CPX. Because CS and CEL are both polysaccharides and have similar structure, it is expected that the release of CPX from them will be similar. Being a protein, KER has a structure that is very much different from that of the polysaccharide.<sup>24,41</sup> In fact, it is known that proteins such as KER have relatively well-defined secondary structure (i.e.,  $\alpha$ -helix and  $\beta$ -sheet)<sup>24,41</sup> compared to polysaccharides which are known to adopt random structure in solution. This, in effect, makes KER structurally denser compared to CEL and CS.

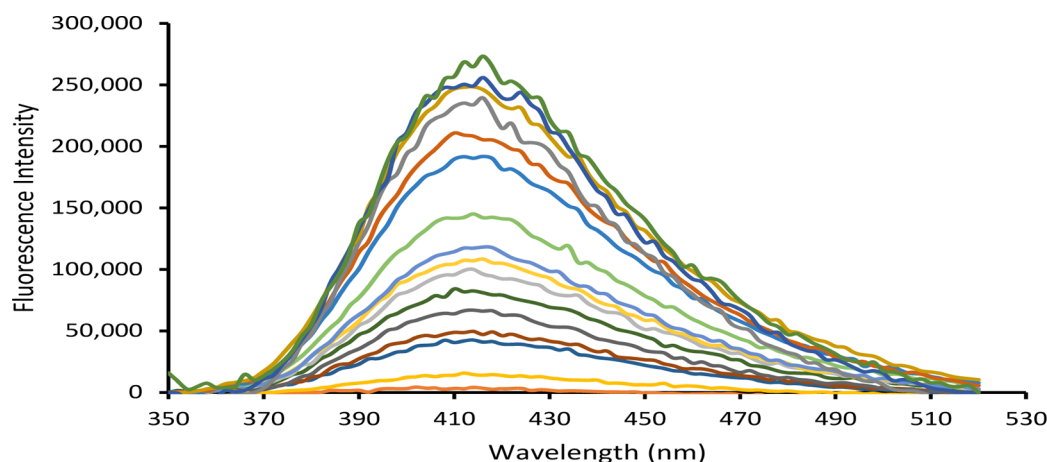


**Figure 3.** Time-dependent fluorescence spectra for Ciprofloxacin release from 100% KER ( $\lambda_{\text{exc}} = 324$  nm).

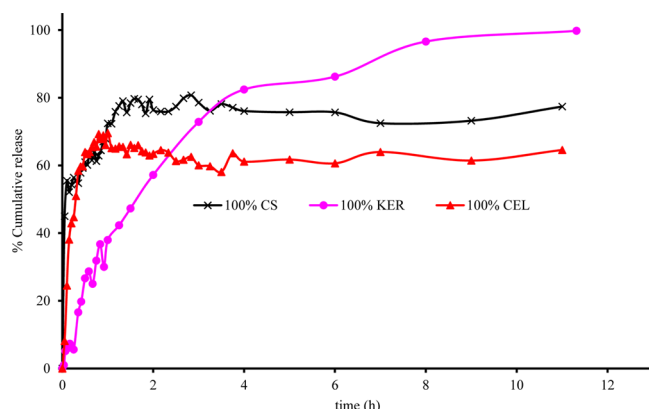


**Figure 4.** Plots of release of CPX as a function of time from 100% CS (black curve with stars), 100% KER (purple curve with filled circles), and 100% CEL (red curve with filled triangles).

Consequently, KER releases the drug at a relatively slower rate than CEL and CS.

Water molecules can diffuse into the biopolymer matrix, producing swelling of the biopolymer. This, in turn, makes it easier for the encapsulated drug to diffuse out and be released. It is known, based on our previous report on swelling,<sup>17</sup> that CS absorbs at least 3 times more water than CEL owing to the more rigid structure of CEL. Therefore, CS is expected to eventually release more drug than CEL at equilibrium. In fact, the results obtained in the present study concur with this finding, namely, 100% CS released a total of 77% CPX whereas 100% CEL released only 65%. Being structurally denser with a well-defined secondary structure, it is expected that it would be relatively harder for water molecules to diffuse into KER.<sup>42</sup>

However, it is possible that the phosphate ions in the buffer may adsorb onto the protein thereby making it more ionic. This, in effect, would make it easier for KER to absorb more water over time. As a consequence, KER released relatively more drug at equilibrium, albeit at a slower pace than either CEL or CS. This could explain why 100% KER released up to 91% of the drug at equilibrium.

As described above, CEL and CS were added to KER to enable [CEL+CS+KER] composites to have better mechanical strength and wider utilization. Releasing profiles of [CEL/CS+KER] composites with different concentrations are shown in Figure 5. In all cases 100% CEL released the least total amount of drug at equilibrium. All samples containing KER showed some degree of controlled release, especially at high KER concentration. Conversely, higher concentrations of either CEL or CS produced the opposite effect. This was most pronounced for composites containing only CEL and CS. As illustrated, all [CS+CEL] composites reached equilibrium within the first hour of the release time. However, when either CEL or CS was blended with KER, there was a substantial slowdown in the rate of drug release. These results clearly indicate that KER can serve in controlling the release of the drug.

#### Quantitative Assessment of the Release Profiles.

Quantitative assessment of the release kinetics was then performed on composites with different compositions and concentrations. This was accomplished by fitting release data to the four kinetic models; zero-order, first-order, Higuchi, and Korsmeyer–Peppas (KP) or power law model. Results obtained of all composites for all models are listed in Table 1. Figure 6 shows representative fitting of the 10:50:40 CS:KER:CEL composite for all four models. The performance of each model was evaluated by visually inspecting the fit and

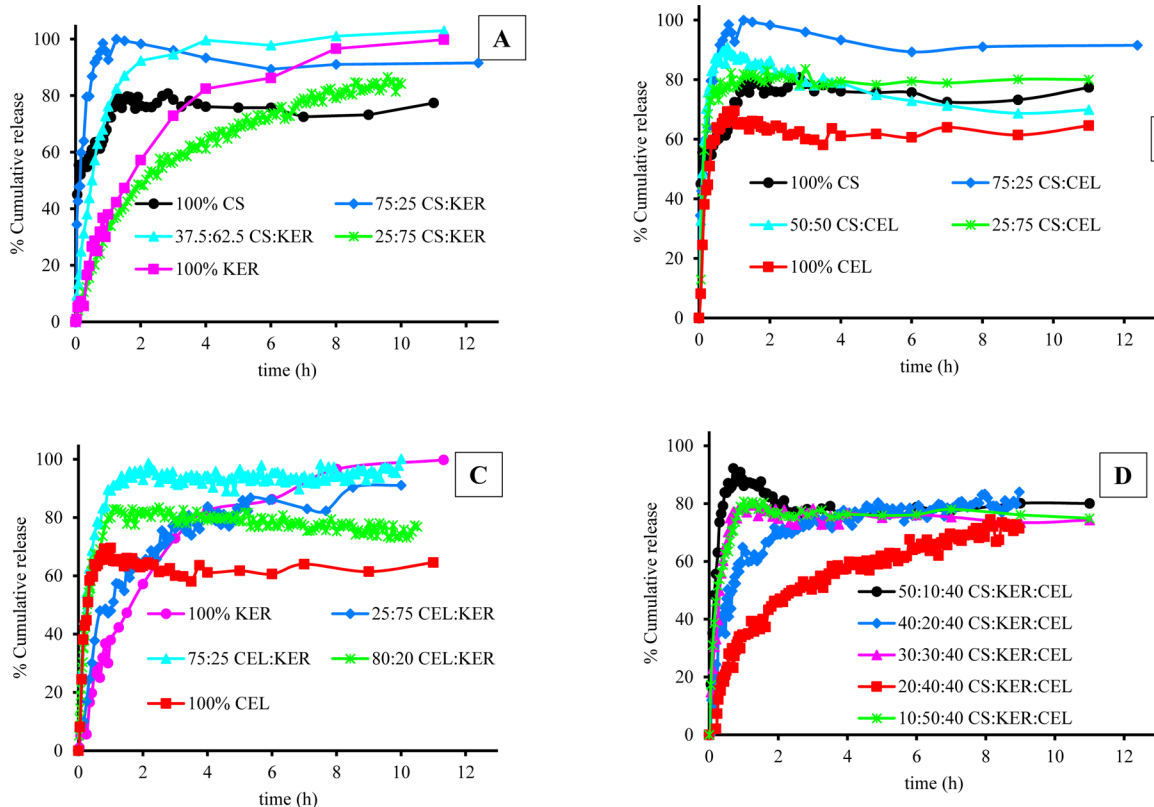


**Figure 5.** Plots of release of CPX as a function of time from (A) [CS+KER], (B) [CS+CEL], (C) [CEL+KER], and (D) [CS+KER+CEL].

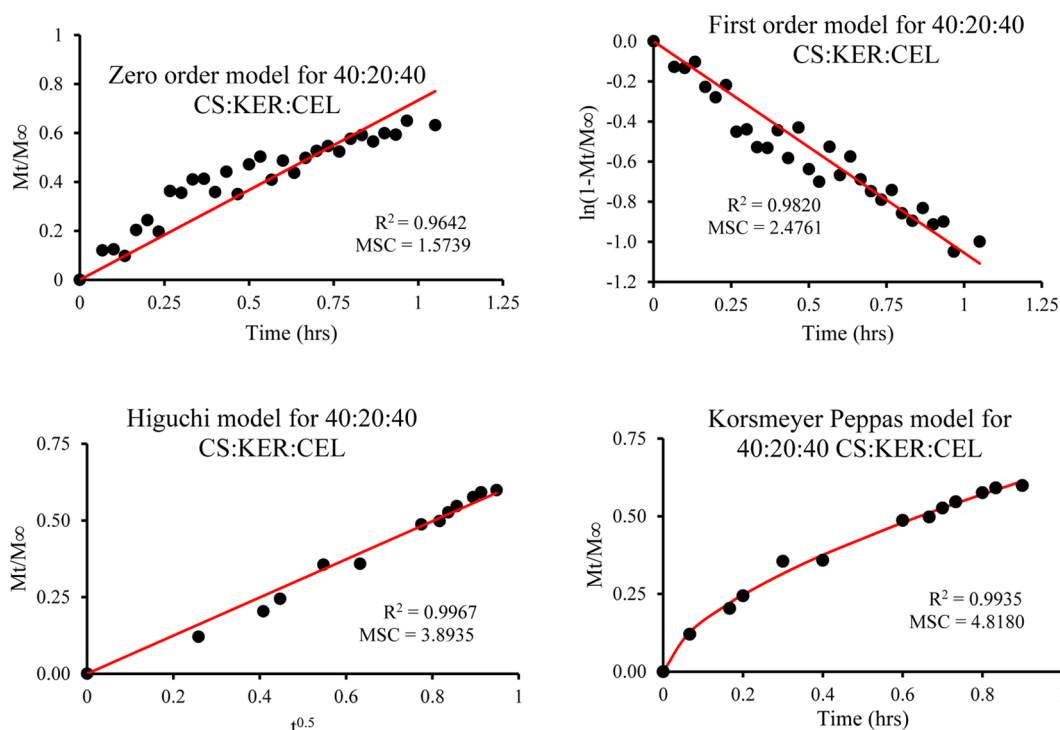


**Figure 6.** Kinetics of release of CPX from 10:50:40 CS:KER:CEL plotted as zero-order, first-order, Higuchi, and Korsmeyer–Peppas or power law model.

the  $R^2$  and MSC values.<sup>43</sup> As shown in Figure 6 and listed in Table 1, data fit very poorly to zero-order model, and, as expected, also gave the lowest  $R^2$  and MSC values for all composites, which indicate that this model cannot be used to describe the release kinetics. Although the first-order model gave relatively better fit and higher  $R^2$  and MSC values for some composites, this trend was inconsistent. For examples, the first-order model gave the highest  $R^2$  and MSC values for only 100% KER, 25:75 CEL:KER, and 50:10:40 and 30:30:40 CS:KER:CEL, which corresponds to only 24% of the total composites measured. It is, therefore, not appropriate either.

Both Higuchi and Korsmeyer–Peppas models have relatively better fit and high values for  $R^2$  with the former having higher values 64% of the time, and the later model 36% of the time. This suggests that both Higuchi and power law models may be suitable. However, when MSC values are also taken into account, the Higuchi model gives higher values of MSC only 24% of the time with the remaining 76% are provided by the Korsmeyer–Peppas model. These two results seem to be contradictory at first. However, closer inspection reveals that that the differences in the  $R^2$  values of both models are relatively small whereas the differences in MSC are substantially larger. As a consequence, the Korsmeyer–Peppas model seems to be more suited and hence was subsequently used to describe release kinetics.

For clarity the rate constants ( $k_{sp}$  values) from the Korsmeyer–Peppas model were used to generate 3D plots which are shown in Figure 7A for two-component composites ([CEL+KER] and [CS+KER]), and Figure 7B for three-component composites ([CEL+CS+KER]). As illustrated, 100% KER gave the lowest  $k_{sp}$  values ( $0.357 \pm 0.006$ ) compared to that of either 100% CEL or 100% CS. In addition, 100% CEL and 100% CS gave almost identical  $k_{sp}$  values ( $1.04 \pm 0.07$  and  $1.06 \pm 0.01$  for 100% CEL and 100% CS, respectively).

As listed in Table 1 and Figure 7A, for [CS+KER] composites,  $k_{sp}$  values decreased concomitantly with the increase in proportional content of KER. For example, adding 62.5% KER to CS reduced  $k_{sp}$  value by 33%. A further 48% reduction was observed when additional 12.5% of KER was added to the 62.5:37.5 KER:CS composite film. The blending of CS and KER is attractive because CS not only improves the mechanical properties but may also provide additional benefits. Specifically, we have previously shown that CS fully retains its unique properties (hemostasis and ability to inhibit the growth of both Gram positive and negative microorganisms (including *Escherichia coli*, *Staphylococcus aureus*, methicillin resistant *S. aureus* and vancomycin resistant *Enterococcus faecalis*) when added to CEL.<sup>16,18</sup> It is, therefore, expected that CS also can retain its property as a component of the [KER+CS] composites. The same trend observed in the release by [CS+KER] composites was also seen in the release by [CEL+KER] composites. This is hardly surprising considering CEL and CS are both polysaccharide and possess similar chemical structure except for the presence of amino groups in CS. However, for a given KER content, the [CEL+KER] composite film gave a  $k_{sp}$  value somewhat higher than that of the corresponding [CS+KER] composite. For example, composites containing 75% KER gave  $k_{sp}$  values of  $0.53 \pm 0.01$  for [CEL+KER] and  $0.313 \pm 0.005$  for [CS+KER]. To verify that KER was indeed responsible for the slowdown in drug release, we synthesized CPX-doped composite films containing only the two polysaccharides, CEL and CS. The kinetic results are listed in Table 1 and plotted in Figure 7A. It is interesting to note that when these two polysaccharides were blended, the resultant composites gave  $k_{sp}$  values that were relatively higher than  $k_{sp}$  values obtained from either 100% CEL or 100% CS. In addition, the  $k_{sp}$  values for the [CS+CEL] composites do not seem to correlate to the amount of either CS or CEL in the composites. This behavior could be a result of similarity in the



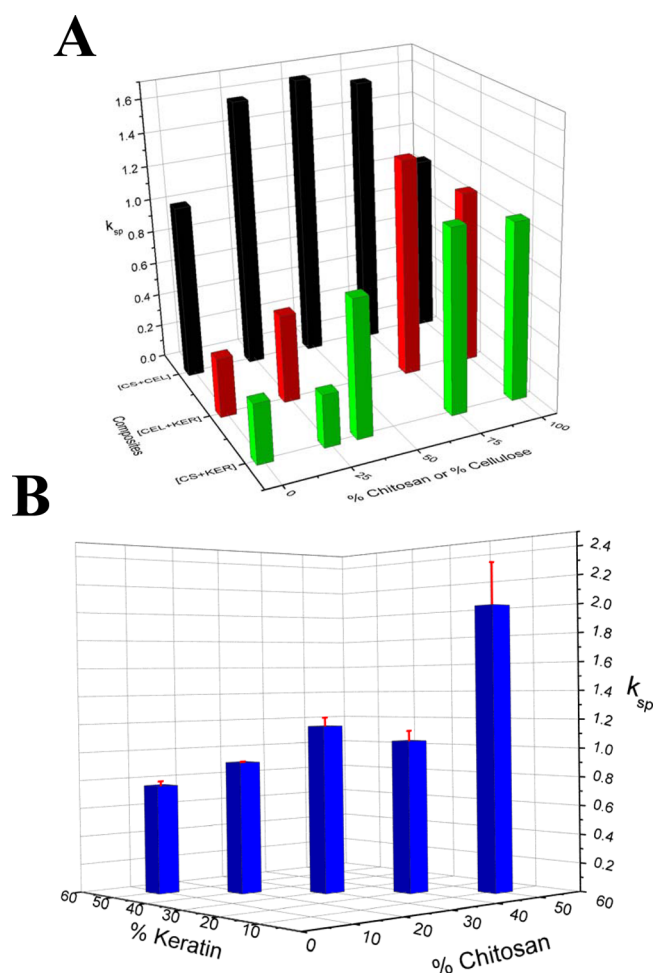


**Figure 7.** 3D plot for release rate constants,  $k_{sp}$ , obtained by fitting release data to Korsmeyer–Peppas model for (A) two-component composites ([CEL+CS] (black), [CEL+KER] (red), and [CS+KER] (green)) and (B) three-component composites ([CS+KER+CEL]).

chemical structures of these two polysaccharides. The fact that the  $k_{sp}$  values for [CEL+CS] composites were consistently higher than  $k_{sp}$  values of either [CEL+KER] or [CS+KER] further confirms the ability of KER to control drug release.

Experiments were also designed to determine if KER can still slow drug release from a composition containing KER, CEL, and CS. Five composites were synthesized in which the concentration of CEL was fixed at 40% whereas those for CS and KER were varied from 10% to 50%. The results are listed in Table 1 and plotted in Figure 7B. Again, it was found that increasing concentration of KER leads to a substantial decrease in the release kinetics. For example, increasing concentration of KER from 10% to 30% leads to a 41% decrease in the release rate (from  $2.0 \pm 0.3$  to  $1.16 \pm 0.06$ ). Further increasing KER concentration to 50% lead to  $k_{sp}$  value of  $0.76 \pm 0.03$  or 34% reduction. It is therefore evidently clear that the ability of KER to slow the release of the drug remains intact in three-component composites as well. This finding is of particular significance because it indicates that drug release can be controlled and adjusted at any rate by judiciously selecting the concentration of KER in the [CEL+CS+KER] composite. Furthermore, the [CEL+CS+KER] composite is superior to all other two-component composites as it has combined properties of all three components, namely, superior mechanical strength

(from CEL); hemostasis, bactericide, and ability to adsorb pollutants and toxins (from CS); and controlled release of drugs (from KER).

Additional information on the mechanism of the drug release can also be obtained from the exponential value ( $n$ ) of the Korsmeyer–Peppas model. As described in the section above, if  $n \leq 0.45$ , the mechanism is Fickian; if  $0.5 \leq n \leq 0.8$ , the mechanism is non-Fickian; and if  $0.8 \leq n \leq 1.0$ , a zero-order mechanism governs the drug release from the composites.<sup>32–35</sup>  $n$  values for different composites are listed in Table 1. With the exception of two composites (75:25 CS:KER and 10:50:40 CS:KER:CEL) which, within experimental error, have  $n$  values close to 0.4, all other 13 composites have  $0.5 \leq n \leq 0.8$ . The results seem to indicate that drug release from these composites is governed mainly by a non-Fickian mechanism. It is possible that more than one mechanism is involved in the release. For example, a combination of diffusion and relaxation of the biopolymers including swelling by water and unfolding of the biopolymers contribute to the releasing of the drug from the composites.

## CONCLUSIONS

We have demonstrated that novel composite materials containing CEL, CS, and KER can be successfully synthesized by a simple, green, and totally recyclable one-step process. Adding CEL into the composite substantially improves its mechanical strength thereby enabling it to be used for practical and general applications. All three biopolymers, CEL, CS, and KER, were found to be able to encapsulate a drug such as ciprofloxacin (CPX) and subsequently release it either as a single or as two- or three-component composites. Interestingly, release rates of CPX by CEL and CS either as a single or as [CEL+CS] composite are relatively much faster and independent of concentration of CS and CEL in the composite. Conversely, releasing rate by KER is much slower, and when incorporated into CEL, CS, or CEL+CS, it substantially slows the release rate of the composites as well. Furthermore, the reducing of the release rate was found to correlate to the concentration of KER in the composite. This may be due to the fact that KER, being a protein, is known to have secondary structure, whereas CEL and CS exist only in random form. This, in effect, makes KER structurally denser compared to CEL and CS, which are porous because of their random structure. Consequently, KER releases the drug at rate that is relatively slower than that of CEL and CS. Taken together, results obtained clearly indicate that drug release can be controlled and adjusted at any rate by judiciously selecting the concentration of KER in the [CEL+KER], [CS+KER], and [CEL+CS+KER] composites. Furthermore, the fact that the [CEL+CS+KER] composite has combined properties of all three components, namely, superior mechanical strength (from CEL), hemostasis and bactericide (from CS), and controlled release of drugs (from KER), indicates that it is possible, for the first time, to use this novel composite for general and practical applications which hitherto have not been possible. This includes its use as a high-performance bandage which can heal wounds, kill bacteria, and deliver drugs for the treatment of chronic ulcerous wounds of diabetic patients.

## ■ ASSOCIATED CONTENT

### ■ Supporting Information

Additional information about the chemicals and instruments used in this work. This material is available free of charge via the Internet at <http://pubs.acs.org>.

## ■ AUTHOR INFORMATION

### Corresponding Author

\*Tel.: 1 414 288 5428. E-mail: [chieu.tran@marquette.edu](mailto:chieu.tran@marquette.edu).

### Notes

The authors declare no competing financial interest.

## ■ ACKNOWLEDGMENTS

Research reported in this publication was supported by the National Institute of General Medical Sciences of the National Institutes of Health under Award R15GM099033.

## ■ REFERENCES

- (1) Verma, V.; Verma, P.; Ray, P.; Ray, A. R. Preparation of scaffolds from human hair proteins for tissue-engineering applications. *Biomed. Mater.* **2008**, *3*, 025007.
- (2) Sando, L.; Kim, M.; Colgrave, M. L.; Ramshaw, J. A.; Werkmeister, J. A.; Elvin, C. M. Photochemical crosslinking of soluble wool keratins produces a mechanically stable biomaterial that supports cell adhesion and proliferation. *J. Biomed. Mater. Res., Part A* **2010**, *95*, 901–911.
- (3) Yamauchi, K.; Maniwa, M.; Mori, T. Cultivation of fibroblast cells on keratin-coated substrata. *J. Biomater. Sci., Polym. Ed* **1998**, *9*, 259–270.
- (4) Hill, P.; Brantley, H.; Van Dyke, M. Some properties of keratin biomaterials: Keratines. *Biomaterials* **2010**, *1*, 585–593.
- (5) Tanabe, T.; Tachibana, A.; Yamauchi, K. Recent Res. *Dev. Protein Eng.* **2001**, *1*, 247–254.
- (6) Saul, J. M.; Ellenburg, M. D.; de Guzman, R. C.; Van Dyke, M. Keratin hydrogels support the sustained release of bioactive ciprofloxacin. *J. Biomed. Mater. Res., Part A* **2011**, *98A*, 544–553.
- (7) Narendra, R.; Qiuran, J.; Enqi, J.; Zhen, S.; Xiuliang, H.; Yiqi, Y. Bio-thermoplastics from grafted chicken feathers for potential biomedical applications. *Colloids Surf., B* **2013**, *110*, 51–58.
- (8) Xiao-Chun, Y.; Fang-Ying, L.; Yu-Feng, H.; Yan, W.; Rong-Min, W. Study on effective extraction of chicken feather keratins and their films for controlling drug release. *Biomater. Sci.* **2013**, *1*, 528–536.
- (9) Vasconcelos, A.; Cavaco-Paulo, A. The use of keratin in biomedical applications. *Curr. Drug Targets* **2013**, *14*, 612–619.
- (10) Cui, L.; Gong, J.; Fan, X.; Wang, P.; Wang, Q.; Qiu, Y. Trans glutaminase-modified wool keratin film and its potential application in tissue engineering. *Eng. Life Sci.* **2013**, *13*, 149–155.
- (11) Xu, S.; Sang, L.; Zhang, Y.; Wang, X.; Li, X. Biological evaluation of human hair keratin scaffolds for skin wound repair and regeneration. *Mater. Sci. Eng., C* **2013**, *33*, 648–655.
- (12) de Guzman, R. C.; Merrill, M. R.; Richter, J. R.; Hamzi, R. I.; Greengauz-Roberts, O. K.; Van Dyke, M. E. Mechanical and biological properties of keratose biomaterials. *Biomaterials* **2011**, *32*, 8205–8217.
- (13) Rouse, J. G.; Van Dyke, M. E. A review of keratin-based biomaterials for biomedical applications. *Materials* **2010**, *3*, 999–1014.
- (14) Songmei, X.; Lin, S.; Yaping, Z.; Xiaoliang, W.; Xudong, L. Biological evaluation of human hair keratin scaffolds for skin wound repair and regeneration. *Mater. Sci. Eng., C* **2013**, *33*, 648–655.
- (15) Battista, O. A.; Smith, P. A. Microcrystalline cellulose. *Ind. Eng. Chem.* **1962**, *54*, 20–29.
- (16) Tran, C. D.; Duri, S.; Harkins, A. L. Recyclable synthesis, characterization, and antimicrobial activity of chitosan-based polysaccharide composite materials. *J. Biomed. Mater. Res., Part A* **2013**, *101*, 2248–2257.
- (17) Tran, C. D.; Duri, S.; Delneri, A.; Franko, M. Chitosan-cellulose composite materials: preparation, characterization and application for removal of microcystin. *J. Hazard. Mater.* **2013**, *252*, 355–366.
- (18) Harkins, A. L.; Duri, S.; Kloth, L. C.; Tran, C. D. Chitosan-cellulose composite for wound dressing material. Part 2. Antimicrobial activity, blood absorption ability, and biocompatibility. *J. Biomed. Mater. Res., Part B* **2014**, *102*, 1199–1206.
- (19) Han, X.; Armstrong, D. W. Ionic Liquids in Separations. *Acc. Chem. Res.* **2007**, *40*, 1079–1086.
- (20) El Seould, O. A.; Koschella, A.; Fidale, L. C.; Dom, S.; Heinze, T. Applications of ionic liquids in carbohydrate chemistry. *Biomacromolecules* **2007**, *8*, 2629–2647.
- (21) Pinkert, A.; Marsh, K. N.; Pang, S.; Staiger, M. P. Ionic liquids and their interaction with cellulose. *Chem. Rev. (Washington, DC, U.S.)* **2009**, *109*, 6712–6728.
- (22) Mora-Pale, M.; Meli, L.; Doherty, TV; Linhardt, RJ. Room temperature ionic liquids as emerging solvents for the pretreatment of lignocellulosic biomass. *Biotechnol. Bioeng.* **2011**, *108*, 1229–1245.
- (23) Rehman, A.; Zeng, X. Ionic Liquids as Green Solvents and Electrolytes for Robust Chemical Sensor Development. *Acc. Chem. Res.* **2012**, *45*, 1667–1677.
- (24) Xie, H.; Li, S.; Zhang, S. Ionic liquids as novel solvents for the dissolution and blending of wool keratin fibers. *Green Chem.* **2005**, *7*, 606–608.
- (25) Schaeffer, A. J. The expanding role of fluoroquinolones. *Am. J. Med.* **2002**, *113* (suppl. 1A), 45S–54S.
- (26) Segev, S.; Yaniv, I.; Haverstock, D.; Reinhart, H. Safety of long term therapy with ciprofloxacin: Data analysis of controlled clinical trials and review. *Clin. Infect. Dis.* **1999**, *28*, 299–308.
- (27) Varelak, C. G.; Dixon, D. G.; Steiner, C. Zero-order release from biphasic polymer hydrogels. *J. Controlled Release* **1995**, *34*, 185–192.
- (28) Costa, P.; Manuel, J.; Lobo, S. Modeling and comparison of dissolution profiles. *Eur. J. Pharm. Sci.* **2001**, *13*, 123–133.
- (29) Gibaldi, M.; Feldman, S. Establishment of sink conditions in dissolution rate determinations. Theoretical consideration and application to non-disintegrating dosage forms. *J. Pharm. Sci.* **1967**, *56*, 1238–1242.
- (30) Wagner, J. G. Interpretation of percent dissolved-time plots derived from in vitro testing of conventional tablets and capsules. *J. Pharm. Sci.* **1969**, *58*, 1253–1257.
- (31) Higuchi, T. Rate of release of medicaments from ointment bases containing drugs in suspension. *J. Pharm. Sci.* **1961**, *50*, 874–875.
- (32) Higuchi, T. Mechanism of sustained-action medication. Theoretical analysis for rate of release of solid drugs dispersed in solid matrices. *J. Pharm. Sci.* **1963**, *52*, 1145–1149.
- (33) Korsmeyer, R. W.; Gurny, R.; Doelker, E. M.; Buri, P.; Peppas, N. A. Mechanism of solute release from porous hydrophilic polymers. *Int. J. Pharm.* **1983**, *15*, 25–35.
- (34) Ritger, P. L.; Peppas, N. A. A simple equation for description of solute release II. Fickian and anomalous release from swellable devices. *J. Controlled Release* **1987**, *5*, 37–42.
- (35) Ritger, P. L.; Peppas, N. A. A simple equation for description of solute release I. Fickian and non-fickian release from non-swellable devices in the form of slabs, cylinders or discs. *J. Controlled Release* **1987**, *5*, 23–36.
- (36) Peppas, N. A.; Sahlin, J. J. A simple equation for the description of solute release. III. Coupling of diffusion and relaxation. *Int. J. Pharm.* **1989**, *57*, 169–172.
- (37) Li, L.; Wang, D. Preparation of regenerated wool keratin films from wool keratin-ionic liquid solutions. *J. Appl. Polym. Sci.* **2003**, *127*, 2648–2653.
- (38) Peplow, P. V.; Roddick-Lanzilotta, A. D. Orthopaedic materials derived from keratin, U.S. Patent 2005/0232963 A1, 2005.
- (39) Fang, J. Y.; Chen, J. P.; Leu, Y. L.; Wang, H. Y. Characterization and evaluation of silk protein hydrogels for drug delivery. *Chem. Pharm. Bull.* **2006**, *54*, 156–162.
- (40) Persson, A. M.; Sokolowski, A.; Pettersson, C. Correlation of in vitro dissolution rate and apparent solubility in buffered media using a miniaturized rotating disk equipment: Part 1. Comparison with a

traditional USP rotating disk apparatus. *Drug Discoveries Ther.* **2009**, *3*, 104–113.

(41) Aluigi, A.; Zoccola, M.; Vineis, C.; Tonin, C.; Ferrero, F.; Canetti, M. Study on the structure and properties of wool keratin regenerated from formic acid. *Int. J. Biol. Macromol.* **2007**, *41*, 266–273.

(42) Reichi, S.; Borrelli, M.; Geerling, G. Keratin films for ocular surface reconstruction. *Biomaterials* **2011**, *32*, 3375–3386.

(43) Phaechamud, T.; Ritthidej, G. Formulation Variables Influencing Drug Release from Layered Matrix System Comprising Chitosan and Xanthan Gum. *AAPS PharmSciTech* **2008**, *9*, 870–877.